APPLICATION OF THE SACRIFICIAL MATERIAL AS A BASE FOR THE MATRIX FOR IMMOBILIZATION OF SPENT NUCLEAR FUEL CONSTITUENTS AT NUCLEAR REACTOR CORE MELT PROGRESSION

V.N. Mineev
Institute of High Temperatures RAS, Izhorskaya st. 11, Moscow, Russia

S.V. Stefanovsky, O.I. Kirjanova
SIA Radon, 7th Rostovskii per. 2/14, Moscow 119121 Russia

B.S. Nikonov
Institute of Geology of Ore Deposits RAS, Staromonetnii 35, Moscow 109017 Russia

A.S. Shulgin
Institute of Chemical Technology, Kashirskoye shosse, 33, Moscow, Russia

ABSTRACT

Materials produced by smelting of a nuclear reactor core surrogate (corium) with sacrificial material based on zirconia and titania in an inductive furnace in a fianite (yttria-stabilized zirconia) crucibles were examined by X-ray diffraction (XRD), scanning electron microscopy with energy dispersive system (SEM/EDS), and electron-probe microanalysis (EPMA). Composition of the corium was chosen from analysis of the results of calculations of various scenarios of heavy accidents for Russian WWER-1000 nuclear reactor (in kg or mass fractions): UO_2 – 75,000; Zr – 17,400; ZrO_2 – 6,351; Fe (stainless steel) – 100,000; Cs – 275; Sr – 44; Pu – 616; Am – 7.4. The batch fed into the crucibles consisted of corium constituents (40 wt.%) and sacrificial material (60 wt.%) composed of ZrO_2, Al_2O_3, BaO, and CaO.

In crucible near-surface area fianite $Zr_{0.67…0.83}Y_{0.17…0.33}O_{1.84…1.92}$ formed due to corrosion of crucible walls was found to be a major phase. In the bulk major phase was zirconia-titania-urania cubic solid solution (natural analog is mineral tazheranite). There are two different ones, one of which is enriched and second of them is depleted with uranium. Moreover iron-containing phases with formulae $FeTiO_3$, $Fe_{0.95}O$, and $Fe_2(Ti,Al)O_{4-x}$ with widely variable Ti:Al ratios were found. Nevertheless, major fraction of iron of stainless steel remained unoxidized and was located as an ingot and drops in the bulk of the material.

Formation of urania-zirconia-titania cubic solid solution with high chemical durability and radiation resistance provides for safe and reliable immobilization of fuel constituents, especially uranium and plutonium, in the case of heavy accident with core melt progression.

INTRODUCTION

As a result of the accident at the fast neutron channel nuclear reactor (Russian abbreviation – RBMK) of the Chernobyl nuclear power plant (NPP), melting of the reactor core and interaction of the melt (“corium”) with reactor materials with formation of so-called “Chernobyl lava” occurred. That “Lava” contained vitreous phase and several crystalline phases including non-

stoichiometric oxide $(Zr,U)O_{2-x}$ and high-uranium zircon $(Zr,U)SiO_4$ [1]. To immobilize the molten corium it was proposed to install special catchers filled with sacrificial material, which is to be reacted with corium to stop melt progression and form a material with high chemical durability, radiation resistance, and strong mechanical integrity providing for safe and reliable immobilization of nuclear fuel constituents [2-6]. Thus, the problem of corium immobilization is rather similar to radioactive waste immobilization. The most promising host phases for actinides and rare earths immobilization are known to be titanates, zirconates and titanozirconates with fluorite-derived structure, in particular cubic zirconia-based solid solution, pyrochlore, and zirconolite capable to accumulate up to ~40-50 wt.% oxides of these elements (in total) [7-10]. Synroc is titanate ceramic proposed for immobilization of high level non-partitioned wastes from commercial nuclear reactors consisting of major (~95%) zirconolite, perovskite and hollandite selectively incorporating fission, corrosion products, fuel constituents and process contaminants [11]. Both Synroc and ceramics based on its constituents may be produced via crystallization of melts containing titanium, zirconium, calcium, rare earths, actinides and some iron group elements oxides [12]. A possibility to apply TiO_2 and ZrO_2-bearing compounds as sacrificial materials of external catcher of nuclear reactor has been confirmed in previous studies [5,6]. These provide for

- increase of melt volume and thus effective surface of heat-exchange between the melt and catcher walls;
- reduction of temperature level in the melt;
- complete oxidation of metallic Zr;
- inverse stratification or, as a final result, homogenization of oxide and metallic constituents of the melt;
- prevention of interaction between water and steel giving rise to threat of vapor explosion and high-rate hydrogen release.

Along with these, application of the TiO_2 and ZrO_2-based sacrificial materials provides for formation of high-stable titanate and zirconate phases capable to incorporate fuel components and fission products. In our previous works [12,13] we have demonstrated formation of perovskite, zirconolite and hollandite at crystallization of the melt containing ZrO_2, TiO_2, Al_2O_3, BaO, CaO.

The goal of the given work is investigation of the process of titano-zirconate matrices formation at cooling of the melt, containing simultaneously UO_2-based corium and the TiO_2-ZrO_2-based sacrificial material, and examination of products including phase composition and elements partitioning determination.

Experimental

Composition of the corium was chosen from analysis of the results of calculations of various scenarios of heavy accidents for Russian WWER-1000 nuclear reactor [14] (in kg or mass fractions): UO_2 – 75,000; Zr – 17,400; ZrO_2 – 6,351; Fe (stainless steel) – 100,000; Cs – 275; Sr – 44; Pu – 616; Am – 7.4. The batch fed into the crucibles consisted of corium constituents (40 wt.%) and sacrificial material (60 wt.%) composed of ZrO_2, Al_2O_3, BaO, and CaO. The calculated batch composition was as follows (in wt.%): stainless steel X18H10T (Fe) – 20.2; UO_2 – 15.1; Zr – 3.5; ZrO_2 – 33.7; TiO_2 – 14.4; Al_2O_3 – 7.0; BaO – 3.8; CaO – 2.3.

Three melting tests were performed in an induction furnace with a process frequency of 1.76 MHz in air in crucibles manufactured from yttria-stabilized cubic zirconia (fianite): outer diameter - 120 mm, wall thickness - 15 mm, bottom thickness – 20 mm. Batches in amounts of 300 (No.1), 400 (No.2) or 600 g (No.2) were fed into crucibles in each of tests, heated to 2700 K at a rate of ~400 K/min, kept at this temperature for 1 hour, and cooled to ~1000 K at a rate of ~10 K/min. High-rate gas release, melt circulation during melting and the amount of crucible corrosion after melting were observed.

Crucibles with solidified melts were coated with epoxy resin to prevent destruction and cut along two diameters followed by fragmentation and examination visually, by X-ray diffraction using a DRON-4 diffractometer (Cu K_α - radiation), and by scanning electron microscopy with energy dispersive system (SEM/EDS) using a JSM-5300+Link ISIS analytical unit. Phases were identified using a JCPDS-ICDD database. Appearance of the fragment of the ingot No.1 and analytical points are also shown on Figure 1. Autoradiographic images were obtained using a standard procedure. Elemental analysis was performed using ICP-MS spectrometry.

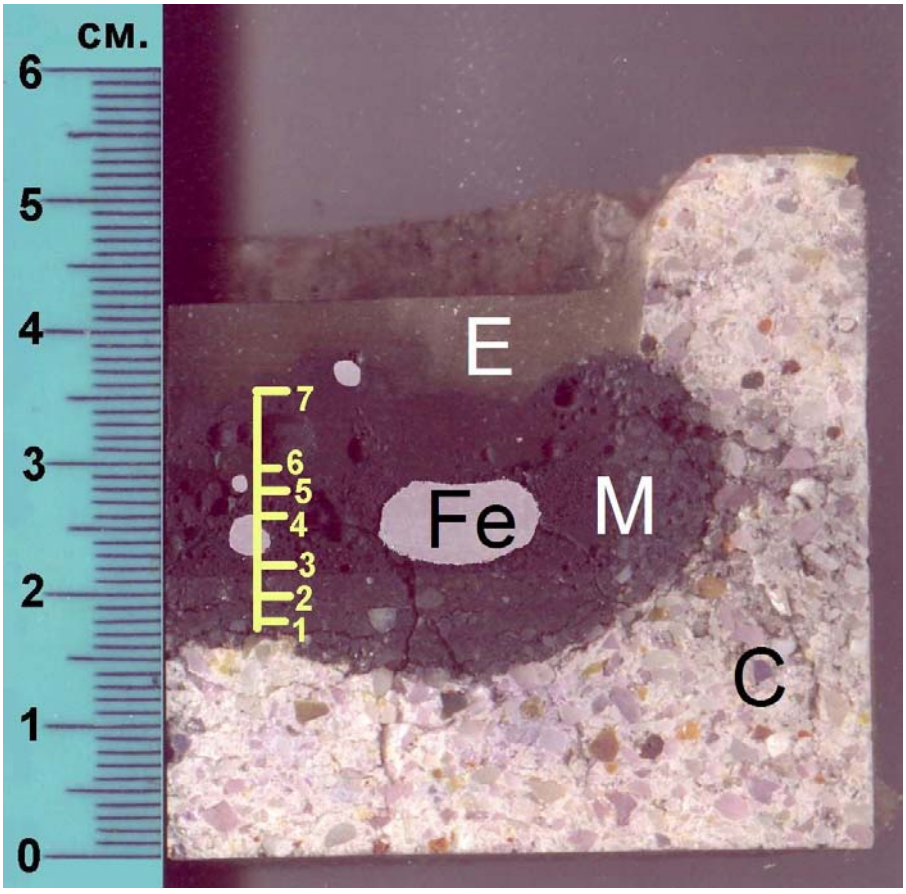

Fig. 1. Vew of the fragment of the ingot No.1 used for analyses. Analytical points are shown on the picture. C - crucible material, M – melt material, Fe – metal inclusions, E – epoxy resin.

Results

As seen from Fig. 1 significant corrosion of crucible walls and bottom occurred during melting. Melting under oxidizing conditions (in air) resulted in complete oxidation of metallic zirconium and incomplete oxidation of metallic iron, a major fraction of which remained in a metallic form and was observed as metallic inclusions with shape close to spherical 1-2 mm in diameter (in the tests Nos. 1 and 2) or plates ~1×5×10 mm in size (in the test No.3). The largest spherical inclusion in the bulk of the solidified melt from the test No.1 was located in the central part of the ingot (Fig. 1). Increase of ZrO_2 content and Y_2O_3 dissolution in the melt due to crucible corrosion also occurred (Table I). In total oxides contents in the ingot and their initial contents in the batch are significantly different due to oxidizing of metallic constituents and corrosion of crucible walls.

XRD patterns of the materials sampled from the ingots produced in the tests Nos.1-3 are free from metallic inclusions as shown on Fig. 2. Phase and elemental compositions in more details were obtained using SEM/EDS. The data are given in Table I.

The material sampled from the near-wall zone of the ingot from the test No.1 (points 1 and 2 on Fig. 1) is composed of fianite (1-1 on Figure 2) whose major reflections (2.9866, 2.5707, 1.8156, 1.5524) almost exactly correspond to reference data for $Y_{0.15}Zr_{0.85}O_{1.93}$ (JCPDS 30-1486). Minor shift of the diffraction peaks positions to lower angles is due to a little bit higher average Y_2O_3 in fianite that is consistent with SEM/EDS data. Analysis of the border zone melt-crucible in the place of the most intense corrosion of the fianite crucible (point 1 on Fig. 1 and Fig. 3, *1*) shows that major phase in this zone is fianite with rather widely variable composition described by formula $Zr_{0.75…0.86}Y_{0.15…0.24}O_{1.84…1.92}$. In the same zone but slightly higher (point 2 on Fig. 1 and Fig. 3, *2*) major phase was also found to be fianite $Zr_{0.80}Y_{0.20}O_{1.90}$ but large (200-300 μm across) rare grains with high hafnium content and impurity of silica (grain 2 on Fig. 3, *2*) occurred. Their composition is recalculated to formula $Hf_{0.53}Zr_{0.07}Y_{0.26}Si_{0.14}O_{1.87}$. Probably hafnium oxide as well as silicon oxide in zircon $ZrSiO_4$ and hafnon $HfSiO_4$ was present as impurity in the source zirconia, which was used to produce fianite being crucible material. Composition of the fianite near the border of this grain corresponds to formula $Zr_{0.70}Hf_{0.01}Ti_{0.01}Y_{0.19}O_{1.88}$.

Zone 3 is in the vicinity of one of the metallic shots (Fig. 3, *3*). Section at the distance from the shot is composed of fianite with averaged formula $Zr_{0.80}Hf_{0.01}Y_{0.19}O_{1.91}$ similar to formula of major fianite of zone 2. Intermediate zone is inhomogeneous. The basis is composed of aggregates with average formula $Zr_{0.50}U_{0.15}Ti_{0.10}Ca_{0.08}Fe_{0.14}Al_{0.03}O_{1.77}$ formed by fluorite-type cubic solid solution whose formula may be calculated as $Zr_{0.63}U_{0.19}Ti_{0.08}Ca_{0.10}O_{1.90}$ and ulvospinel type phase with formula $Fe_2(Ti_{0.57}Al_{0.43})O_{3.79}$. Metallic shot consists of predominant iron ((95 wt.%) and traces of other stainless steel constituents (point 3 on Fig. 3, *3*, and Fig. 4).

Analysis of the intermediate zone in more details (Fig. 3, *4*) confirms that its major bulk is composed of fluorite-type cubic solid solution with fine (<10 μm) grains iron titanate, aluminotitanate or oxide (wuestite) distributed within. Two varieties of cubic solid solutions with different Zr:U ratios differed in color on SEM-images co-exist: enriched and depleted with uranium with formulae $U_{0.57…0.69}Zr_{0.21…0.33}Hf_{0.00…0.01}Ca_{0.06…0.08}O_{1.93…1.96}$ (points 1 and 5 on Fig. 3, *4*) and $U_{0.14…0.20}Zr_{0.67…0.73}Ti_{0.01…0.07}Ca_{0.07…0.12}O_{1.89…1.93}$ (points 2 and 3 on Fig. 3, *4*),

Table I. Chemical Composition of the Phases in the Ingot No.1 by SEM/EDS Data.

Oxides	Points on Fig. 1 / points on Fig. 3																							
	1/1		2/2			3/3			3[1]/4					4/6				5/7	6/8		7/9			
	1	2	1	2	3	1	2	3[2]	1	2	3	4	5	1	2	3	4	1	1	2	1	2	3	4
Al_2O_3	-	-	-	-	-	-	0.8	0.5	1.5	-	1.1	9.2	-	0.5	0.8	13.1	13.3	-	10.9	1.0	-	7.5	1.0	0.7
SiO_2	-	-	-	5.1	-	-	-	2.8	-	-	-	-	-	-	-	-	-	-	-	-	-	-	1.0	-
P_2O_5	5.5	2.6	4.1	-	-	2.9	-	-	-	-	-	-	-	-	-	-	-	-	-	-	-	-	-	-
CaO	-	0.5	-	-	-	-	2.9	-	1.1	4.4	2.4	1.0	1.9	3.4	3.4	-	0.3	2.9	0.5	4.5	4.7	1.8	3.8	6.9
TiO_2	-	-	-	-	-	-	4.9	-	3.6	11.2	2.2	18.1	-	1.0	1.9	22.0	19.3	1.6	14.5	6.9	10.5	10.3	8.1	3.9
MnO	-	-	-	-	-	-	-	0.2	-	-	-	-	-	-	-	0.4	0.4	-	0.9[3]	-	-	0.5[3]	-	-
FeO	-	-	-	-	-	-	6.4	95.4	4.9	7.5	5.0	45.1	-	3.9	5.9	60.4	59.7	3.6	69.6	78.1	4.4	51.5	5.5	6.0
NiO	-	-	-	-	-	-	-	0.2	-	-	-	-	-	-	-	-	0.5	-	-	-	-	-	-	-
Y_2O_3	23.6	11.6	16.1	17.7	18.2	14.7	-	-	-	-	-	-	-	-	-	-	-	-	-	-	-	-	-	-
ZrO_2	72.2	83.7	77.7	4.9	72.0	77.1	39.3	-	9.4	49.8	48.2	15.4	20.7	63.7	54.8	6.5	-	64.1	-	3.9	43.0	8.6	38.6	43.8
BaO	-	-	-	-	-	-	-	-	2.2	2.0	-	-	-	-	-	-	-	-	-	-	20.2	-	15.2	2.3
HfO_2	-	-	-	66.4	2.5	1.3	-	-	-	-	-	-	-	-	-	-	-	1.7	-	1.0	-	-	-	-
UO_2	-	-	-	-	-	-	26.3	-	67.4	22.2	29.4	8.4	77.9	29.4	27.2	-	-	23.3	-	0.7	21.1	11.1	16.5	34.0
Total	101.3	98.4	97.9	94.1	92.7	96.0	80.6	99.1	90.1	97.1	88.3	97.2	100.5	101.9	94.0	102.4	93.5	97.2	96.4	96.1	103.9	91.3	89.7	97.6
Phase[4]	F	F	F	F+H+ Hn	F	F	Z	Fe	U+S	Z+S	Z+S	S	U	Z	Z	S	S	Z	S	S+W	Z+B	S+Z	Z+B	Z+S

[1] detail; [2] metal, composition is given in at.%; [3] Cr_2O_3; [4] B – barium titanate or zirconate, F – fianite, H – hafnium oxide (HfO_2), Hn – hafnon ($HfSiO_4$), S – spinels, U – UO_2 –based cubic solid solution (uraninite); W – wuestite (FeO_{1-x}) Z – ZrO_2-based cubic solid solution.

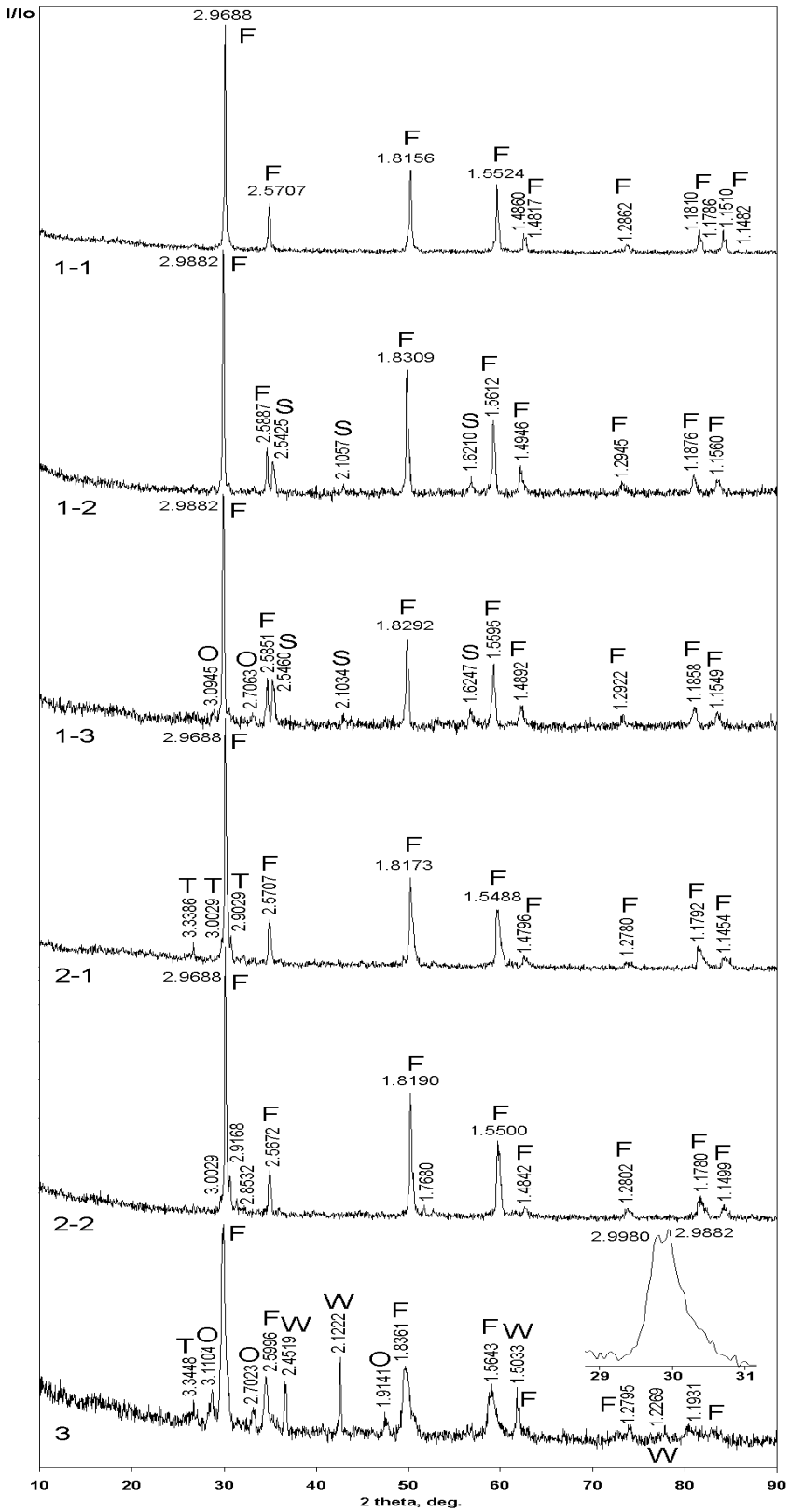

Fig. 2. XRD patterns of the samples. F – fianite or fluorite-type cubic phase, O – UO_2-based cubic phase, S – spinels, T – non-stoichiometric titanium oxides (Magneli phases), W – wustite.

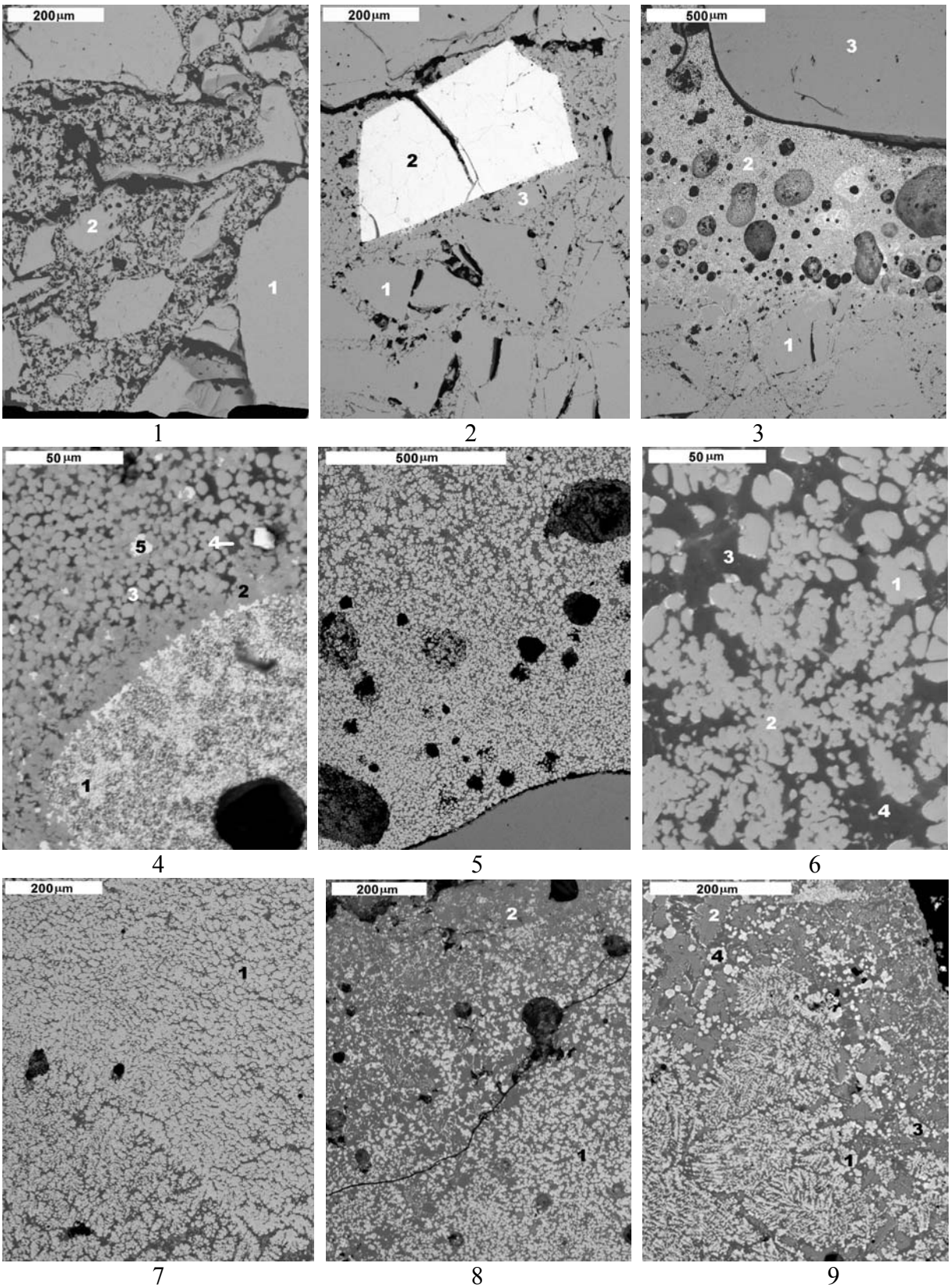

Fig. 3. SEM-images of the samples. Analytical points are shown on Fig. 1. Compliance between analytical points and pictures is given in the text and Table I.

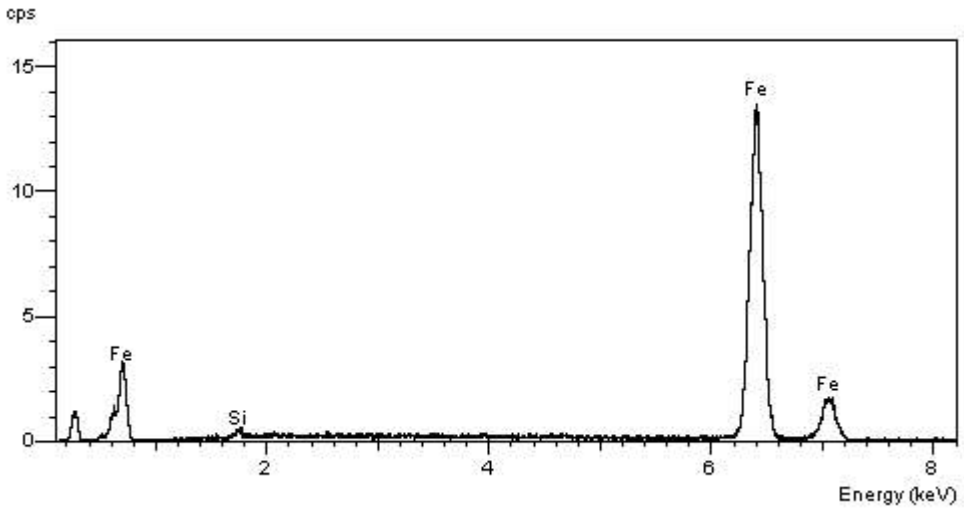

Fig. 4. EDX spectrum of the metallic inclusion (shot) from the ingot No.1.

respectively. Composition of iron-containing inclusions varies from almost stoichiometric $FeTiO_3$ and $Fe_{0.95}O$ to $Fe_2(Ti,Al)O_{4-x}$ with wide variation of Ti:Al ratio.

The next (on height) zone (*4* on Fig. 1 and Fig. 3, *5*,*6*) is composed of two phases – zirconia-based cubic solid solution with impurity of iron and other iron group elements (corrosion products) and generalized formula $Zr_{0.65}U_{0.14}Ti_{0.03}Ca_{0.08}Fe_{0.09}Al_{0.01}O_{1.83}$ (lighter grains) and iron aluminotitanate $Fe_{1.80}Ti_{0.54}Zr_{0.09}Al_{0.57}O_{3.92}$ (darker grains). It is possible that iron is present in the cubic solid solution as separate phase (wuestite) distributed as very fine (<5 μm) inclusions in the major bulk.

Averaged composition of zone 5 (Fig. 1 and Fig. 3, *7*) being recalculated to the formula of the cubic solid solution is approximately the same as in the zone 4: $Zr_{0.71}U_{0.12}Ti_{0.03}Ca_{0.07}Fe_{0.07}O_{1.86}$. It is seen that the bulk is inhomogeneous and it is actually cubic solid solution (light on SEM image) containing fine iron-bearing inclusions (dark on SEM image).

XRD pattern of the material sampled from the section of the ingot located between points 3 and 5 on Fig. 1 shows predominant cubic phase whose major reflections (2.9882, 2.5887, 1.8309, 1.5612, etc.) may be attributed to zirconia-urania based fluorite-type cubic solid solution (1-2 on Fig. 3) that is consistent with SEM/EDS data. Spinelides as additional phase are responsible for reflections at 2.5425, 2.1057 and 1.6210 Å (approximately correspond to JCPDS 25-417 card).

Zone 6 (Fig. 1 and Fig. 3, *8*) is located near iron shot and composed of major iron-containing phases with minor cubic solid solution. Composition of one of the iron-bearing phases is close to ulvospinel $Fe_{2.04}Ti_{0.39}Zr_{0.06}Al_{0.45}Cr_{0.03}Ca_{0.03}O_{3.72}$. The second phase is wuestite $Fe_{0.82}Ca_{0.06}Ti_{0.06}Al_{0.01}O$.

Finally, the sample from the highest located zone (*7* on Fig. 1) is also composed of several phases. One of them is fluorite-type cubic solid solution with variable composition. Its major bulk is some enriched with zirconium relatively to uranium and described by formula $Zr_{0.68}U_{0.15}Ca_{0.17}O_{1.83}$ (points 1 and 3 on Fig. 3, *9*), the other occurred as individual larger grains is enriched with uranium: $Zr_{0.59}U_{0.21}Ca_{0.20}O_{1.80}$ (point 4 on Fig. 3, *9*). Fine (<10 μm) barium

titanate $BaTiO_3$ crystals are present in interstitials or as aggregates with grains of the fluorite-type cubic solid solution. Ulvospinel grains containing traces of uranium and zirconium and described by formula $Fe_{1.89}Ti_{0.33}Al_{0.39}Zr_{0.18}U_{0.12}Cr_{0.03}Ca_{0.06}O_{3.84}$ are predominant at the edge of this zone. XRD pattern (1-3 on Fig. 2) of the material sampled from the ingot in the section between points 6 and 7 (Fig. 1) contains reflections typical of fluorite-type cubic solid solution (2.9882, 2.5851, 1.8292, 1.5595 Å and others) and weaker reflections attributed to spinel-type phase (2.5460, 2.1034, 1.6247 Å) as well as two weak peaks which can be due to fluorite-type cubic solid solution enriched with UO_2 that is in a good agreement with SEM/EDS data.

XRD patterns of two sections of the ingot produced in the test No.2 show that ZrO_2-based cubic phase with major reflections at 2.9688, 2.5672-2.5707, 1.8173-1.8190, 1.5488-1.5500 Å and others (2-1 and 2-2 on Fig. 2) is predominant. Minor phase is probably non-stoichiometric titanium oxides TiO_{2-x} responsible for reflections at 3.3386, 3.0029, 2.9029-2.9168 Å.

XRD pattern of the sample from the ingot produced in the test No.3 demonstrates domination of cubic phase (probably two varieties) responsible for peaks at 2.9980 and 2.9982 (components of the strongest reflection), 2.5996, 1.8361, 1.5643 Å and others. Splitting is characteristic of both the strongest and the rest of peaks. Moreover, minor cubic phase responsible for reflections at 3.1104, 2.7023 and 1.9141 Å is also present. The intermediate in abundance phase is wuestite (2.1222, 2.4519, 1.5033, and 1.2269 Å). Traces of non-stoichiometric titanium oxides (Magneli phases) probably responsible for peak at 3.3448 Å occurred. It is clear that the ingot is compositionally inhomogeneous due to insufficient time for melt homogenization resulting in co-existence of three fluorite structure phases with different ZrO_2:UO_2 ratios. Reflection at d_{111} = 3.1104 is due to cubic solid solution with the highest uranium content whose composition is close to uraninite. The phase with the lowest UO_2 content is responsible for peak at d_{111} = 2.9882 Å. From comparison with the samples 1-2 and 1-3 of the ingot No.1 uranium content may be estimated as 0.12-0.14 formula units. The phase whose the strongest reflection corresponds to d_{111} = 2.9980 Å has intermediate composition.

Thus, in the whole in ingot No.1 the predominant phase is fianite or fluorite-type cubic solid solution (natural analog is mineral tazheranite [15]). Minor ulvospinel-type iron-containing phases are also present. In ingot No.2 the major phase is cubic solid solution based on ZrO_2 and probably UO_2, and minor phases are titanium oxides (Magneli phases). In ingot No.3 the major phase is cubic solid solution, the secondary in abundance phase is wuestite $Fe_{0.95}O$, and minor phase is UO_2-based cubic solution (uraninite). Total content of extra phases do not exceed ~20 vol.%. No amorphous phase was found in any samples.

As follows from the authoradographic study, uranium oxide in the whole is quite homogeneously distributed over the bulk of the samples. Its amount was reduced due to dilution of the melt with zirconia. However, as described above, it was found in different phases: in fianite in the near-wall zone and in fluorite-type cubic solid solution in the bulk.

Discussion

As follows from XRD and SEM/EDS data, all three ingots consist of three zones and inclusions:

- crucible corrosion zone composed mainly of crucible material phase – fianite;
- intermediate zone with predominant fluorite-type cubic solid solution with variable composition, where sections both enriched with ZrO_2 and enriched with UO_2 are present;

- near-surface zone also composed mainly of fluorite structure phase but iron-containing phases as well;
- metallic shots (>95% Fe) surrounded by layer enriched with iron which is formed by iron-containing phases (ulvospinel, iron aluminotitanate, wuestite).

However, in all three ingots the predominant phases are fianite and fluorite-type cubic solid solution whose natural analog is mineral tazheranite [15]. As it has been shown by numerous investigations (see, for example, [7-13,16-20] the phases with fluorite and fluorite-derived structures (pyrochlore, murataite, zirconolite) are efficient hosts for actinides and rare earths. One of these phases – murataite, except capability to concentrate actinides (in the Synroc-type ceramic for immobilization of rare earth-actinide fraction of FSUE “PA Mayak” 5 vol.% murataite accumulates >40 wt.% of total uranium in the sample [10]), is a host phase for iron group elements (corrosion products) [16] as well. Fluorite-type cubic phases have very high chemical durability and the highest radiation resistance among the candidate phases for HLW and excess weapons plutonium immobilization [8-10]. At that, fluorite structure phases are the most hardly amorphized. The samples were not rendered amorphous even after ion-irradiation to 300 displacements per atom (dpa) at room temperature [19] and 110 dpa at 90 ^{0}C [20]. This shows that fluorite structure phases will remain stable for geological periods necessary to for decay even the longest-lived actinides and, therefore, this means practically “eternal” immobilization of corium components in the sacrificial material, although it is more correct to speak about formation of safe and reliable matrix from the corium and sacrificial material. If to take into account that fluorite-type cubic solid solutions have maximum possible ranges of homogeneity (complete miscibility), for example, cubic (*Fm3m*) ZrO_2, UO_2, and PuO_2 form continuous solid solutions, all the restrictions on chemical composition of such matrices should be lifted. Because cesium and strontium radionuclides contents are approximately 0.1% and 0.02% of corium mass respectively (these correspond to ~0.05 wt.% and <0.01 wt.% in the matrix) their effect on the structure and properties of matrices is negligible. At such low concentrations these elements may enter various crystalline phases as isomorphic impurities in amount of ≤0.01 formula units. They may be also present in interstitial glass whose content in the samples studied is so low that it was not found neither XRD nor SEM/EDS analyses.

CONCLUSION

New ceramic formulation composed of fluorite-type cubic solid solution (fianite, tazheranite) as major phase and iron-containing minor phases suitable for molten nuclear reactor core immobilization has been produced using inductive melting. Uranium as major corium component is incorporated in the fluorite structure phase, which has high chemical durability and radiation stability and can serve as safe and reliable immobilizing matrix. The results obtained demonstrate possibility to confine molten corium constituents (fuel components and fission products) in the matrix based on TiO_2 and ZrO_2 as sacrificial material.

REFERENCES

1. B.E. BURAKOV, E.B. ANDERSON, S.I. SHABALEV, et al., Mat. Res. Soc. Symp. Proc. 465 (1997) 1297.
2. A.S. SIDOROV, A.B. NEDOREZOV, M.F. ROGOV, et al., “Issues of safety of NPP with WWER”. Proc. Sem., St-Petersburg, Russia Sept. 12-14, 2000.
3. M. FISCHER, Proc. OECD Workshop on Ex-Vessel Debris Coolability. Karlsruhe, Nov. 15-18, 1999, p. 508-517.
4. M. NIE, Ibid., p. 527-534.
5. V.N. MINEEV, F.A. AKOPOV, A.A. AKOPIAN, et al., Atomic Energy (Russ.) 90 [6] (2001) 460.
6. V.N. MINEEV, F.A. AKOPOV, A.S. VLASOV, et al., Atomic Energy (Russ.) 93 [5] (2002) 348.
7. S.V. YUDINTSEV, B.S. NIKONOV, S.V. STEFANOVSKY, Proc. Int. Conf. on Future Nuclear Systems Global ’99, Jackson Hole, August 29 – September 3, 1999. CD-ROM.
8. W.J. WEBER, R.C. EWING, Mat. Res. Soc. Symp. Proc. 713 (2002) 443.
9. J. LIAN, S.V. YUDINTSEV, S.V. STEFANOVSKY, et al., Mat. Res. Soc. Symp. Proc. 713 (2002) 461.
10. S.V. STEFANOVSKY, Y.M. KULYAKO, S.V. YUDINTSEV, et al., Iss. Rad. Safety. (Russ.) [1] (2002) 15.
11. A.E. RINGWOOD, S.E. KESSON, E.J. RAMM, Radioactive Waste Forms for the Future. Amsterdam, Elsevier, 1988, p. 233-334.
12. S.V. STEFANOVSKY, B.S. NIKONOV, B.I. OMELIANENKO, et al., Phys. Chem. Mat. Treat. (Russ.) [6] (1997) 111.
13. I.A. SOBOLEV, S.V. STEFANOVSKY, F.A. LIFANOV, Radiochem. (Russ.) 35 (1993) 99.
14. I.V. KUKHTEVICH, V.V. BEZLEPKIN, V.S. GRANOVSKY, et al., Heat Power Engin. (Russ.) [9] (2001) 2.
15. R.K. RASTSVETAEVA, D.Y. PUSCHAROVSKY, E.M. SPIRIDONOV, and V.M. GEKIMIANTZ, Rep. Acad. Sci. (Russ.) 359 (1998) 529.
16. N.P. LAVEROV, I.A. SOBOLEV, S.V. STEFANOVSKY, et al., Rep. Acad. Sci. (Russ.) 362 (1998) 670.
17. S.V. STEFANOVSKY, S.V. YUDINTSEV, B.S. NIKONOV, et al., Mat. Res. Soc. Symp. Proc. 556 (1999) 27.
18. N.P. LAVEROV, B.I. OMELIANENKO, S.V. YUDINTSEV, and B.S. NIKONOV, Geol. Ore Deposits (Russ.) 38 (1996) 387.
19. W.L. GONG, W. LUTZE, R.C. EWING, Mat. Res. Soc. Symp. Proc. 556 (1999) 63.
20. L.M. WANG, S. ZHU, S.X. WANG, and R.C. EWING, Mat. Res. Soc. Symp. Proc. 663 (2001) 293.